

## Effect of particle size on the magnetization process in lithographic arrays of Nd<sub>2</sub>Fe<sub>14</sub>B

著者	安藤 康夫
journal or publication title	Journal of applied physics
volume	87
number	9
page range	6325-6327
year	2000
URL	<a href="http://hdl.handle.net/10097/35840">http://hdl.handle.net/10097/35840</a>

doi: 10.1063/1.372694

# Effect of particle size on the magnetization process in lithographic arrays of $\text{Nd}_2\text{Fe}_{14}\text{B}$

Hitoshi Kubota, Takayuki Ikari, Yasuo Ando, Hiroaki Kato, and Terunobu Miyazaki

Department of Applied Physics, Tohoku University, Aoba-yama 08, Aramaki, Aoba-ku, Sendai 980-8579, Japan

Controlled arrays of  $\text{Nd}_2\text{Fe}_{14}\text{B}$  were fabricated via sputtering and lithography. The arrays were fabricated via optical and electron-beam lithography combined with dry etching technique. Designed particle size varies from  $10\ \mu\text{m} \times 10\ \mu\text{m}$  to  $0.5\ \mu\text{m} \times 0.5\ \mu\text{m}$ . We found an increase in the coercive field with decreasing particle size. Results of the micromagnetic calculations suggest that the coercive-field increase in smaller-sized particles is originated from the effective decrease in the exchange-coupling energy owing to the relative increase in the fraction of surface grain. © 2000 American Institute of Physics. [S0021-8979(00)74608-1]

## I. INTRODUCTION

There has been much interest in artificially engineering the magnetic properties of the thin magnetic films by lithographic structuring.<sup>1-3</sup> The ability to design and control magnetic properties is very useful not only from a technological point of view, but also opens up the possibility of experimentally studying fundamental magnetic properties of the material. The experimental study of the magnetic properties of microfabricated magnets are focused mainly on soft magnetic materials. Smyth *et al.*<sup>1,2</sup> have reported that, in permalloy particles, the coercive field  $H_c$  increase with decreasing particle size. They explained the results by taking account of the change in the switching mechanism.<sup>2</sup> As for the hard magnets, only one report<sup>4</sup> exists as far as we know, although the magnetization process is expected to change more significantly than in soft magnets. Since the characteristic length scale such as critical size of single-domain particle is larger than that in soft magnets and reaches the submicron range, we can observe the effect of the particle size on their magnetic properties more easily in hard magnets. In the present work, controlled arrays of  $\text{Nd}_2\text{Fe}_{14}\text{B}$  were fabricated via sputtering and lithography. The effect of particle size on the magnetic properties has been examined by magnetization measurements and micromagnetic calculations.

## II. EXPERIMENT

The films of Ti(50 nm)/ $\text{Nd}_2\text{Fe}_{14}\text{B}$  (500 nm)/Ti(50 nm) were synthesized by rf magnetron sputtering on the thermally oxidized Si substrates at an Ar pressure of 0.8 Pa. They were then annealed at 923 K for 30 min under a pressure of  $6 \times 10^{-4}$  Pa. Designed particle size varies from  $10\ \mu\text{m} \times 10\ \mu\text{m}$  to  $0.5\ \mu\text{m} \times 0.5\ \mu\text{m}$  with the constant spacing of  $10\ \mu\text{m}$ . Optical lithography was used for over  $1\ \mu\text{m}$  particles, which was combined with the Ar ion milling technique. Electron-beam lithography was utilized for smaller particles, which was combined with the reactive ion etching (RIE) with  $\text{CF}_4 + \text{H}_2$  mixture and the Ar ion milling technique. We used the  $\text{SiO}_2$  film as a hard mask, because the selectivity of the negative resist for electron-beam lithography to Ti and  $\text{Nd}_2\text{Fe}_{14}\text{B}$  films is very low for the Ar ion

milling. The RIE was used to remove the  $\text{SiO}_2$  layer ( $1.2\ \mu\text{m}$ ) of the trilayer. Since the size of the array was  $5\ \text{mm} \times 5\ \text{mm}$ , the total number of particles varied from  $5 \times 10^4$  to  $2 \times 10^5$  depending on the particle size. The phase structure was checked by x-ray diffraction (XRD) measurements with  $\text{CuK}\alpha$  radiation. The artificial periodic structures formed were observed by SEM. Magnetization curves were measured by a SQUID magnetometer at room temperature in fields of up to 50 kOe which was applied parallel to the array surface.

## III. RESULTS AND DISCUSSION

By means of the XRD measurements, the films were confirmed to be randomly oriented polycrystals of  $\text{Nd}_2\text{Fe}_{14}\text{B}$  and the averaged grain size to be about 15 nm in diameter, which are consistent with our previous report.<sup>5</sup> Figure 1

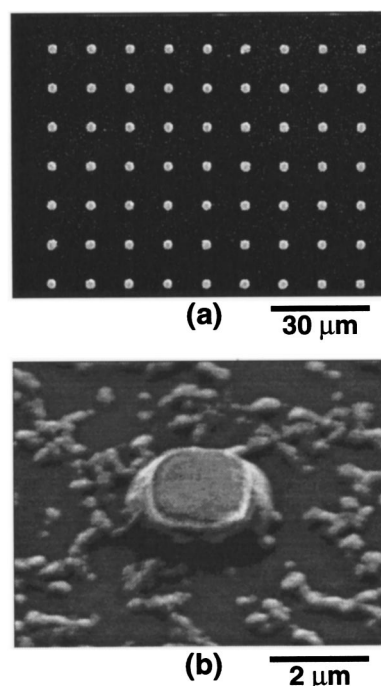


FIG. 1. SEM image of a particle array with the particle size of  $2 \times 2\ \mu\text{m}^2$ .

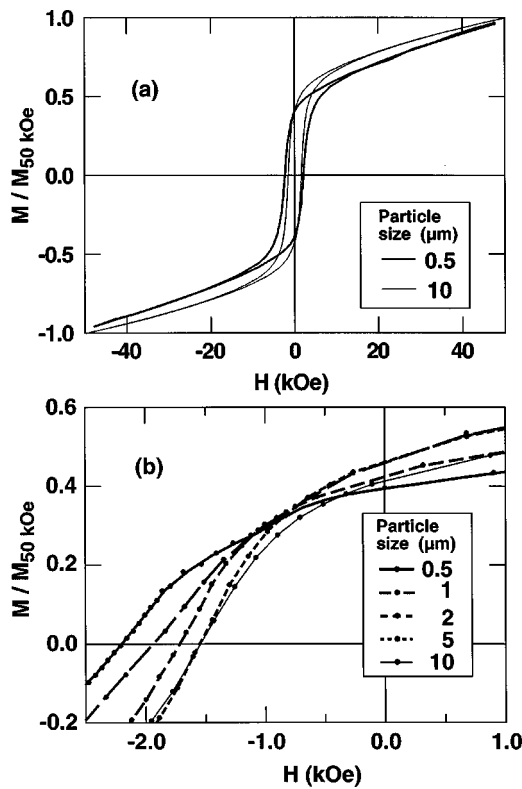


FIG. 2. Magnetization curves of the particle arrays with different particle size. (a) Full loops and (b) demagnetization curves.

shows the SEM image of a particle array with particle size of  $2 \times 2 \mu\text{m}^2$ . The  $\text{Nd}_2\text{Fe}_{14}\text{B}$  particles show a clear periodic structure as shown in Fig. 1(a). Expanded image in Fig. 1(b) shows that observed shape of each particle is rounded in the corner, although the designed shape has been square. This rounding was found to be more significant in smaller-sized particles. The surface around the particle is very rough, which is often observed after ion milling process. Since the milling time was enough to remove the bottom Ti layer, the surface of the substrate is partly etched around the particles.

Figure 2(a) shows the magnetization curves of the particle arrays. Magnetization values are normalized by those at 50 kOe. The overall shape of the curves were found to be almost unchanged. The magnetization values do not saturate even at 50 kOe, although those for increasing and decreasing fields coincide for fields higher than about 20 kOe. The magnitude of  $H_c$  for the  $10 \mu\text{m}$  particle was confirmed to be almost the same as that of the film before microfabrication. With decreasing particle size,  $H_c$  increases systematically from 1.5 kOe ( $10 \mu\text{m} \times 10 \mu\text{m}$ ) to 2.2 kOe ( $0.5 \mu\text{m} \times 0.5 \mu\text{m}$ ) as shown in Fig. 2(b).

In order to interpret the size dependence of  $H_c$ , we have made a micromagnetic calculation. The calculation is based on the method of LaBonte.<sup>6</sup> A cubic particle with a side dimension  $L$  is considered, which consists of cubic cells. Each cell was assumed to represent a  $\text{Nd}_2\text{Fe}_{14}\text{B}$  grain with a size of 15 nm. The number of the cell thus depends on  $L$ , which, for example, is  $100 \times 100 \times 100$  for  $L = 1.5 \mu\text{m}$ . The total energy  $E$  of the system is assumed to be expressed by

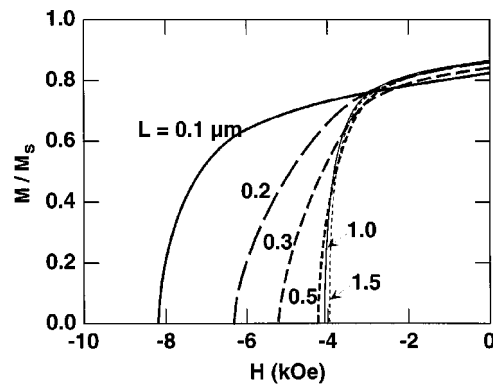


FIG. 3. Calculated magnetization curves for different values of  $L$ .

$$E = \sum_{\text{pair}} A [(\nabla m_x)^2 + (\nabla m_y)^2 + (\nabla m_z)^2] + K_1 \sin^2 \theta - \mathbf{M} \cdot \mathbf{H}, \quad (1)$$

where the first, second, and third terms denote the exchange energy between neighboring grains, anisotropy energy of each grain, and Zeeman energy, respectively. The magnetization vector  $\mathbf{M} = M_s(m_x, m_y, m_z)$  was assumed to be uniform with each cell. The magnitudes of anisotropy constant  $K_1$ , saturation magnetization  $M_s$ , and exchange stiffness constant  $A$  are taken<sup>7,8</sup> to be  $K_1 = 4.3 \times 10^7 \text{ erg/cm}^3$ ,  $M_s = 1.3 \times 10^3 \text{ emu/cm}^3$ , and  $J_e = 16 \text{ erg/cm}^2$ , in which a relation  $A = J_e \cdot \delta h$ , where  $\delta h$  is the intergrain distance, was used. For computational economy, dipolar interactions are ignored, since they are considered to give unimportant contribution owing to the large anisotropy of the system.<sup>8</sup> We have actually checked the effect of dipolar interactions on the coercivity for several choice of  $L$  values. The reduction of  $H_c$  by the inclusion of dipolar interactions was found to be less than 5%, which did not depend on  $H_c$ .

Calculated magnetization curves for different values of  $L$  are shown in Fig. 3. It is seen that remanence value do not depend on  $L$  very much, while  $H_c$  significantly increases with decreasing  $L$ . We have then plotted  $H_c$  as a function of  $L$ , together with the observed  $H_c$ , as shown in Fig. 4. It

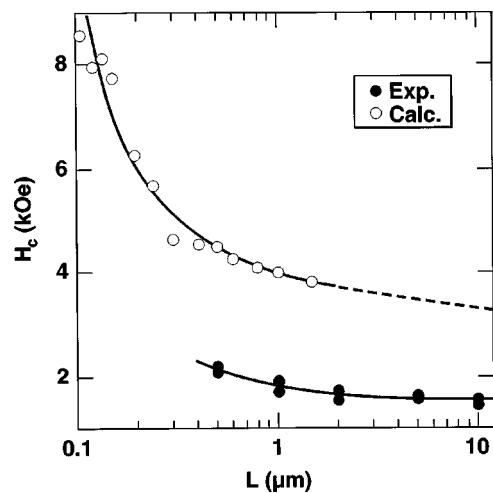


FIG. 4. Experimental and calculated coercive fields  $H_c$  as a functions of  $L$ .

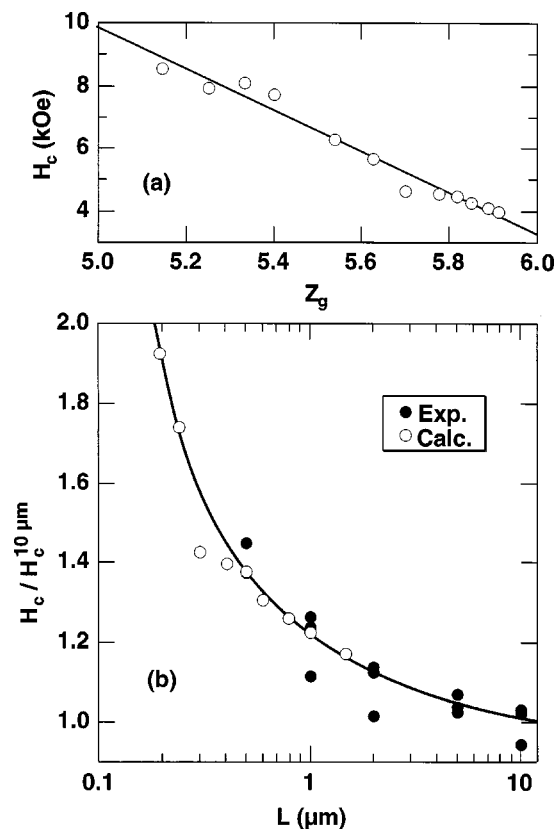


FIG. 5. (a) Calculated  $H_c$  as a function of the average number of neighboring grains  $Z_g$ . (b) Normalized coercive fields as a function of  $L$ .

should be noted that the calculated  $H_c$  is systematically larger than the observation. This difference is considered to come from the simplified modeling of present calculation, in which any possibility of incoherent magnetization changes within the grains and domain wall motion is neglected.<sup>9</sup> Although overlapped range of  $L$  for calculated and observed  $H_c$  is narrow, it appears that  $L$  dependence of  $H_c$  is similar with each other. In smaller-sized particles, a ratio of surface to volume becomes larger, which would modify the exchange

coupling between grains. We thus examined the effect of neighboring grain number on the  $H_c$  value. For example, a number of neighboring grains is six for grains inside a particle, while for surface grains it becomes less than six. In general, the average number of neighboring grains  $Z_g$  is equal to  $6x^2(x-1)/x^3 = 6 - (6/x)$  for each particle with  $x \times x \times x$  cubic grains. In Fig. 5(a), calculated  $H_c$  values given in Fig. 4 are replotted against  $Z_g$ , which are found to give linear dependence with  $Z_g$ . By using this plot, the extrapolated value of the calculated  $H_c$  for the  $10 \mu m$  particle was derived as 3.3 kOe. Figure 5(b) shows the  $L$  dependence of observed and calculated  $H_c$ , both of which are normalized by the  $10 \mu m$  values. Calculated values appear to connect smoothly with the observation. This result thus suggests that the effective decrease in the exchange coupling enhances the independence of randomly oriented grains, which results in the increase of  $H_c$  in smaller-sized particles.

This research is partly supported by Grant-in-Aids for Scientific Research (Priority Areas No. 09750003) from the Ministry of Education, Science, Sports and Culture of Japan, by the Mazda Foundation, and by the Iketani Science and Technology Foundation. A part of this research was performed in the Venture Business Laboratory in Tohoku University.

<sup>1</sup>J. F. Smyth, S. Schultz, D. Kern, H. Schmid, and Dennis Yee, *J. Appl. Phys.* **63**, 4237 (1988).

<sup>2</sup>J. F. Smyth, S. Schultz, D. R. Fredkin, D. P. Kern, S. A. Rishton, H. Schmid, M. Cali, and T. R. Koehler, *J. Appl. Phys.* **69**, 5262 (1991).

<sup>3</sup>A. Maeda, M. Kume, T. Ogura, and K. Kuroki, *J. Appl. Phys.* **76**, 6667 (1994).

<sup>4</sup>H. Lemke, T. Lang, T. Goddenhenrich, and C. Heiden, *J. Magn. Magn. Mater.* **148**, 426 (1995).

<sup>5</sup>M. Shindo, M. Ishizone, H. Kato, T. Miyazaki, and A. Sakuma, *J. Magn. Magn. Mater.* **161**, L1 (1996).

<sup>6</sup>A. E. LaBonte, *J. Appl. Phys.* **40**, 2450 (1969).

<sup>7</sup>T. Schrefl, R. Fischer, J. Fidler, H. Kronmüller, and J. Fidler, *J. Appl. Phys.* **76**, 7053 (1994).

<sup>8</sup>H. Fukunaga and H. Inoue, *Jpn. J. Appl. Phys.* **31**, 1347 (1992).

<sup>9</sup>M. K. Griffiths, J. E. L. Bishop, J. W. Tucker, and H. A. Davis, *J. Magn. Magn. Mater.* **183**, 49 (1998).